APPLIED AND ENVIRONMENTAL MICROBIOLOGY, Nov. 1991, p. 3248–3254
0099-2240/91/113248-07$02.00/0

Vol. 57, No. 11

Alteration of the Magnetic Properties of *Aquaspirillum magnetotacticum* by a Pulse Magnetization Technique†

JUAN C. DIAZ RICCI,[1] BARBARA J. WOODFORD,[1] JOSEPH L. KIRSCHVINK,[1]* AND MICHAEL R. HOFFMANN[2]

Division of Geological and Planetary Science[1] and Division of Engineering and Applied Science,[2] California Institute of Technology, Pasadena, California 91125

Received 28 May 1991/Accepted 26 August 1991

The presence of a narrow shape and size distribution for magnetite crystals within magnetotactic organisms suggests strongly that there are species-specific mechanisms that control the process of biomineralization. In order to explore the extent of this control, cultures of *Aquaspirillum magnetotacticum* in the exponential growth phase were exposed to increasing magnetic pulses with the aim of separating cell populations on the basis of their magnetic coercivities. Isothermal remanent magnetization and anhysteretic remanent magnetization studies were performed with freeze-dried magnetic cells after the remagnetization treatment. Subpopulations of *A. magnetotacticum* that showed an increase in coercivity correlated with the intensity of the magnetic pulses were isolated. After successive subcultures of the remaining north-seeking cells, a maximum bulk coercivity (H_b^{max}) of 40 mT was obtained after treatment with a 55-mT pulse. Although we obtained *A. magnetotacticum* variants displaying higher coercivities than the wild-type strain, changes in crystal size or shape of the magnetite crystals were below reliable detection limits with transmission electron microscopy. Attempts to shift the coercivity towards higher values caused it to decrease, a change which was accompanied by an increase in magnetostatic interactions of the magnetosome chains as well as an increase in the cell population displaying an abnormal distribution of the magnetosome chains. Ultrastructural analyses of cells and magnetosomes revealed the appearance of cystlike bodies which occasionally contained magnetosomes. The increase in cystlike cells and abnormal magnetosome chains when higher magnetic pulses were used suggested that magnetosomes were collapsing because of stronger interparticle magnetostatic forces.

In the 10 years since *Aquaspirillum magnetotacticum* was reported and characterized (1, 2, 20), the discovery of other magnetotactic microorganisms that make differently sized and shaped magnetite (Fe_3O_4) crystals has shown that the crystallographic and magnetic features of the crystals are species specific (3, 17, 22, 25, 26, 28). From a technological point of view, it would be highly desirable to define the mechanisms involved in the bioprecipitation of magnetite in order to be able to control the shape and size of these single-domain particles. Unfortunately, the regulatory mechanisms involved in magnetite biomineralization are unknown, and we do not know how organisms are able to control precisely the precipitation processes.

Several techniques borrowed from the field of rock and mineral magnetism (e.g. that of O'Reilly [24]) have been applied successfully to study magnetic characteristics of these organisms (2). Among them, isothermal remanent magnetization (IRM) and anhysteretic remanent magnetization (ARM) are particularly useful, since they allow the measurement of coercivities and magnetostatic interaction among single-domain chains, providing information about crystal sizes (13). By using these techniques in conjunction with transmission electron microscopy (TEM), it was demonstrated that *A. magnetotacticum* shows a single-chain distribution of 17 to 23 single-domain particles (cuboidal; 50-nm average side length) with a coercivity of about 30 mT (5, 18).

Kalmijn and Blakemore (12) reported that an applied magnetic pulse of higher intensity than the natural coercivity force (H_b) induced the complete reversal of the magnetotactic direction without affecting the viability of the cells (11). This coercive force (or coercivity) is the minimum field strength required to flip the magnetic moment of a uniform magnetized (single-domain) crystal from one stable direction to another. As it is clear that the magnetic polarity is transmitted to the daughter cells (11, 17), we explored the possibility that the pulse remagnetization technique could be used iteratively to enrich populations of bacteria with a desired coercivity. We have isolated successfully subpopulations of *A. magnetotacticum* displaying higher coercivities than the wild-type strain by taking advantage of the inhomogeneous nature of the microbial population. Magnetometric analyses were complemented by TEM observation in order to evaluate any morphological change induced in the cell population.

MATERIALS AND METHODS

Microorganism and culture conditions. Pure cultures of *A. magnetotacticum* ATCC 31632 were obtained from the American Type Culture Collection (10). North-seeking bacteria were always separated magnetically and used for subsequent inocula (2). The cells were grown microaerobically in a chemically defined medium (4). The medium contained the following ingredients (in grams per liter): succinic acid, 0.37; tartaric acid, 0.37; sodium acetate, 0.05; ascorbic acid, 0.035; sodium nitrate, 0.12; and monobasic phosphate, 0.68. The medium was supplemented with 10 ml of Wolfe's vitamin solution (29), 5 ml of Wolfe's mineral solution (29), and 0.005 g of resazurin (all per liter of medium). Ferric quinate was used as the main iron source at

* Corresponding author.
† Contribution no. 5026 of the Division of Geological and Planetary Science.

20 μM. The pH of the medium was adjusted to 6.75 with sodium hydroxide, and the medium was sterilized for 20 min at 120°C. The bacterial cultures were grown in 150-ml screw-cap flasks at 30°C until the exponential phase was reached (optical density at 540 nm = 0.1). They were then pulse remagnetized as described below and subsequently grown until the stationary phase under the effect of an ~2-mT magnetic field produced by a pair of small stirring bar magnets. This small magnetic field allowed the magnetic separation of the south-seeking from the north-seeking subpopulations. The north-seeking bacteria accumulated and concentrated close to the south pole of a magnet, forming a pellet which was harvested aseptically. Part of this magnetic pellet of north-seeking organisms was used to inoculate the next enrichment for the following pulse remagnetization experiment, and the remainder was used for the TEM and magnetometric analyses.

Pulse magnetizer apparatus and experiment. Theoretically, the application of a magnetic pulse antiparallel to the magnetosome chain of a magnetotactic bacterium will cause its magnetic moment to reverse direction if its coercivity happens to be less than the peak field of the pulse. Hence, it would be possible to isolate such bacteria by allowing the bacteria to separate into groups of north- and south-seeking organisms after the pulse. Bacteria with coercivities lower than the magnetic pulse would be remagnetized, and cells having higher coercivities would eventually keep their original magnetotactic preference (12).

The pulse magnetization device used in these experiments was similar to that described by Kirschvink (13). A uniform background biasing magnetic field of 0.4 mT (~10× Earth strength) was produced by using a system of four coils (14, 16) to hold all bacterial cells in a parallel alignment. A second, separate Helmholtz coil pair was configured with a silicon-controlled rectifier-controlled capacitive discharge circuit (13) so as to produce a short (~1-ms) magnetic pulse directed antiparallel to the biasing field. The amplitude of this pulse could be controlled precisely between 0 and 100 mT and was calibrated to within 1% by using a memory Hall probe.

These experiments were carried out using pulses of between 40 and 80 mT. Sealed flasks containing *A. magnetotacticum* grown until the mid-exponential phase were exposed for 5 min to the low, steady, biased magnetic field and were subsequently shot with the antiparallel magnetic pulse.

Electron microscopy. TEM was used for (i) the direct observation of magnetic bacteria and (ii) ultrastructure analysis with sections of fixed and plastic-embedded bacterial cell pellets. For whole cells, cell suspensions were placed directly on grids coated with 0.5% Parlodion (nitrocellulose) in ethyl acetate and were allowed to air dry. These preparations were observed in a Zeiss 9 transmission microscope for analyses of magnetosome chains and for counting the number of magnetosomes per cell.

For thin sections, bacteria were centrifuged at 14,000 rpm (Eppendorf microcentrifuge) for 5 min and washed twice with phosphate buffer (50 mM; pH 7.0). Supernatants were discarded, and the pellet was fixed with 3.6% glutaraldehyde in cacodylate buffer (0.1 M) for 1 h and was postfixed in 1% osmium tetroxide for 1 h. The pellet was dehydrated in a graded series of ethanol concentrations and then in propylene oxide. The dehydrated pellet was embedded in epoxy resin (Polybed; Polyscience, Inc.). Thick and thin sections were cut on a Reichert OMU2 ultramicrotome, stained with uranyl acetate and lead citrate, and viewed with a Zeiss 9 TEM.

Magnetometry. In a single-domain crystal, the direction of the magnetic moment is usually held fixed in one of two stable orientations, either parallel or antiparallel to the particle's long axis. The bulk coercivity, or simply the coercivity (H_b), is the minimum external magnetic field level at which the transition from one direction of the magnetic moment to the antiparallel one takes place. If a sample is exposed briefly to an external magnetic field stronger than the coercivity of some fraction of its magnetic grains, moments of this weaker fraction flip their directions to that closest to the applied field, leaving a net magnetization. As this magnetization is acquired at one temperature, it is called an IRM. Measurements of the IRM remaining after each of a series of progressively stronger magnetic field exposures is one method of measuring the coercivity distribution of a sample. Likewise, a sample can be demagnetized by exposing it to a sinusoidally alternating magnetic field in a process called alternating-field (Af) demagnetization. Repeated application of this procedure with a zero magnetic background field and progressively increasing peak Af levels provides another method of measuring the coercivity distribution of a sample. Finally, if a sample is subjected to an Af demagnetization cycle in the presence of a weak but steady magnetic field, it gains a magnetic moment termed an ARM. The magnitude of the ARM relative to the total IRM is a sensitive indicator of the packing geometry and arrangement of magnetic crystals (7). Isolated crystals or linear chains gain ARM strongly in weak biasing fields, whereas dense highly-interactive aggregations acquire only weak ARM. For further explanations, we recommend the volume by Thompson and Oldfield (27).

Freeze-dried magnetically grown cells (10 to 20 mg) were used for the IRM, Af demagnetization of IRM, and ARM experiments, in which several techniques developed for the study of rocks' mineral magnetism were used (9). The coercivity of a sample was determined by using IRM and Af demagnetization of IRM spectra and particle magnetostatic interactions by ARM. The magnetometer used was a radio-frequency-biased superconducting quantum interference device designed to measure the total magnetic moment of a sample held in an ultra-low-field environment (9). A microcomputer controlled this instrument, as well as a small stepping motor, the magnetic pulse circuit, a biasing coil for the ARM acquisition, and the Af demagnetization system. Af demagnetization was carried out by a linearly decaying inductive capacitive (LC) oscillating circuit in a magnetically shielded coil. IRM acquisition experiments were done by applying increasing magnetic pulses to initially demagnetized samples and measuring the total magnetic remanence after each pulse. Demagnetization plots were obtained by applying incrementally higher alternating magnetic fields until the magnetic remanence of the samples was completely removed. The peak magnetic fields used in these demagnetization studies varied from 0 to 100 mT, with increasing increments of 2.5 mT per demagnetization experiment. ARM analysis was performed on initially demagnetized samples by using a stepwise increment of 0.2 mT from 0 to 2 mT. IRM, Af demagnetization of IRM, and ARM curves were normalized to the maximum value of IRM of each sample. The plots of IRM and Af demagnetization of IRM versus the externally applied magnetic field were used to determine the sample coercivities (H_b) and ARMs for the magnetostatic interaction analyses.

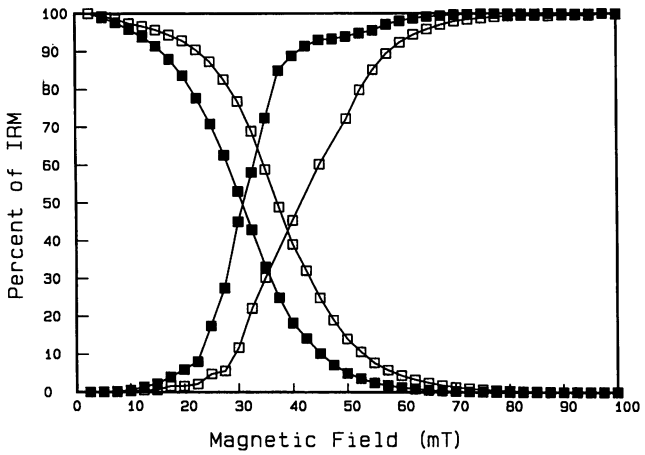

FIG. 1. IRM and Af demagnetization of the IRM curves of the wild-type strain (■) and 55-mT coercivity enrichment (□) of *A. magnetotacticum*. The IRM and Af demagnetization of IRM are normalized to the maximum value of IRM determined for each sample. The magnetic field strength is expressed in milliteslas (1 mT = 10 gauss).

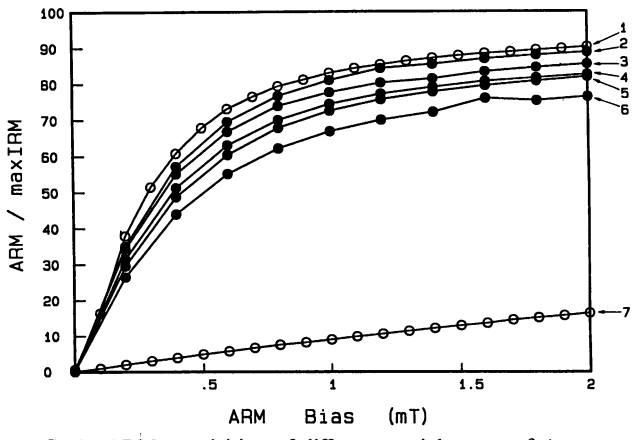

FIG. 3. ARM acquisition of different enrichments of *A. magnetotacticum* after the pulse remagnetization treatment. Open circles represent the characteristic pattern displayed by noninteractive single-domain particles obtained from *A. magnetotacticum* curve 1 and fully interactive single-domain particles from chiton teeth (7) (curve 7). The ARM curve of the wild-type strain of *A. magnetotacticum* overlapped with the uppermost curve (curve 1). Curves 2 to 6 represent the ARMs observed in samples obtained after 40, 50, 60, 70 and 80 mT of pulse remagnetization, respectively. ARM values along the ordinate were also normalized to the maximum IRM value for each sample.

RESULTS

Figure 1 shows results for the acquisition and demagnetization of IRM obtained for wild-type *A. magnetotacticum*. These data show a mean coercivity of 30 ± 1 mT (the abscissa of the intersection point is the best estimate of H_b), which agrees with previous reports for this organism (23). The intersection of the acquisition and demagnetization curves takes place at approximately 50% of the maximum IRM value, which indicates the presence of noninteractive single-domain particles (7, 13, 23). Figure 1 also shows the new magnetic spectra for a subculture of *A. magnetotacticum* measured after five cycles of pulse remagnetization and regrowth. This magnetic pattern was obtained after a 55-mT remagnetization pulse and yielded the maximum coercivity achieved during these experiments (40 mT). Note also that the IRM acquisition and demagnetization have a lower crossing point (45%), indicating that changes in the organization of the single-domain particles led to increased interparticle interactions (discussed further below).

Using the coercivity values determined from the magnetic patterns of each culture enrichment, we obtained the data shown in Fig. 2. With increasing strength of the magnetic pulse, the measured coercivity of the subpopulations of *A. magnetotacticum* first increased and then decreased. Starting with values of coercivity normally found in the wild-type strain (H_b = 30 mT), a maximum value (H_b^{max}) of 40 ± 1 mT was reached after the 55-mT pulse treatment. Although we continued with this pulse remagnetization treatment schedule up to 80 mT, we were unable to shift the coercivity of subsequent populations towards higher values. On the contrary, the magnetic patterns of these enrichments showed decreasing coercivities until they acquired almost the original value (H_b = 32 ± 1 mT). Although the new populations showed higher coercivities than the parental strain during the first phase of the curve (Fig. 2, 30 to 55 mT), their measured coercive force was always less than that of the pulse. We attributed this behavior to the imperfect separation of north- and south-seeking organisms. However, the sustained increase of the coercivity of subsequent enrichments indicated that it is possible to select subpopulations of *A. magnetotacticum* by their spontaneous magnetic differentiation, and these differences were inherited by subsequent generations of microorganisms. The second phase of the curve shown in Fig. 2 suggests that a further increase of the mean coercivity is not possible under these experimental conditions with *A. magnetotacticum*. When enrichments were remagnetized at a pulse strength higher than 60 mT, we always observed a decrease of the coercivity of the resulting population. When the new lower-coercivity enrichments were pulsed again at 55 mT, we obtained the same results as those shown in Fig. 2, indicating either that the rate of randomization of the magnetic properties of the magnetosomes is higher than the growth rate of the higher-coercivity cells or that higher remagnetization pulses alter a more fundamental mechanism involved in the control of the synthesis of magnetite. When the cultures were remagnetized at 75 and 80 mT, the final coercivities approached the values observed for the wild type (Fig. 2).

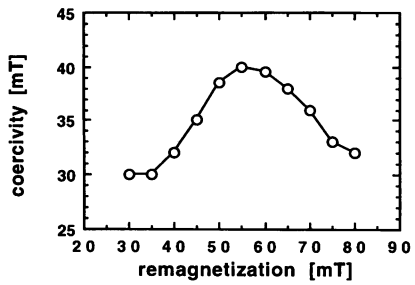

FIG. 2. Effect of the pulse remagnetization technique on the median coercivity of cultures of *A. magnetotacticum*. As discussed in the text, north-seeking cultures of *A. magnetotacticum* were exposed at increasing magnetic pulses, reisolated, and grown and had their coercivity distribution measured.

To investigate the consequences of these magnetic treat-

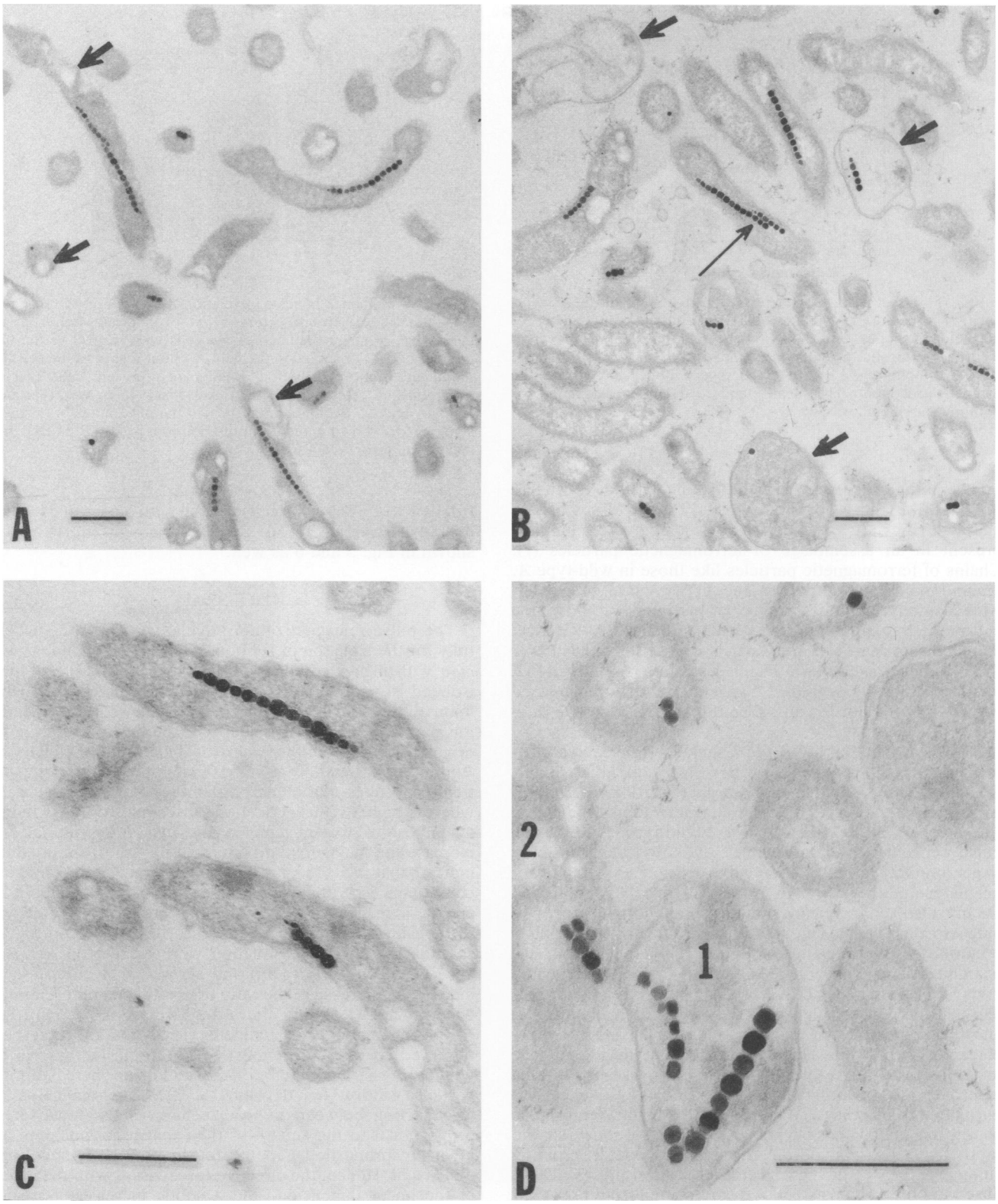

FIG. 4. Transmission electron micrographs of *A. magnetotacticum*. (A) Magnetotactic spirilla exposed to pulse remagnetization of 45 mT. Bacteria appear as curvilinear rods in longitudinal section or as circles in cross section. Most cells contain relatively long chains of magnetosomes (average, 15 magnetosomes per cell) and large granules of poly-β-hydroxybutyrate (arrows) (19). (B) Microphotography of the sample of magnetotactic spirilla after 65-mT remagnetization treatment. Some normal-appearing cells contain double chains (thin arrows), and others appear as large, circular cystlike or irregular profiles (thick arrows) containing fewer or no magnetosomes. (C) Higher magnification of the wild-type strain with variations in length of magnetosome chains visible in plane of section. (D) Large irregular bodies observed in higher-coercivity enrichments of *A. magnetotacticum* (80 mT). The magnetosome chain appears to double back on itself in region 1, and there is a double chain in region 2. Bars, 0.5 μm.

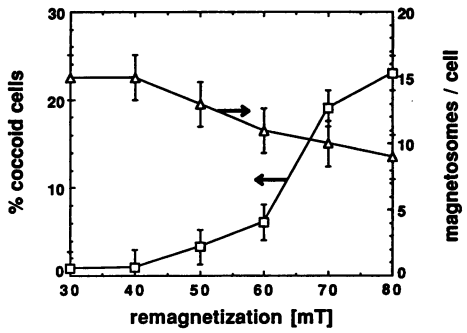

FIG. 5. Effect of the remagnetization treatment on the appearance of coccoid or cystlike cells (□) and average number of magnetosomes per cell (△). For the minimization of the error incurred during the calculation of these data, sets of ten or more separate photos were evaluated for every 10-mT increase of the magnetic treatment. The mean standard deviation calculated for both measurements was σ_{n-1} = 3.2 mT.

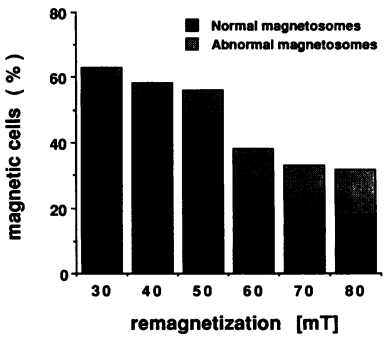

FIG. 6. Influence of remagnetization treatment on the magnetosome chains of *A. magnetotacticum*. Total bars represent the percentage of magnetosome-bearing cells with respect to the total number of cells observed in the field, without regard to the cell type or magnetosome distribution. Solid bars represent cells carrying magnetosome chains similar to those observed in wild-type cells (Fig. 4A and C). Shaded bars represent the percentage of magnetosome chains showing abnormal distributions (Fig. 4B and D). The mean total error was 4%.

ments on the cells, we carried out studies of the ARM (Fig. 3) and TEM (Fig. 4) of the samples. The ARM acquisition characteristics are very sensitive to the degree of clumping present in an assemblage of ferromagnetic particles (7). Chains of ferromagnetic particles like those in wild-type *A. magnetotacticum* plot along the upper curve of Fig. 3, whereas densely packed clumps of particles like those in a chiton tooth (7) plot along the bottom curve (Fig. 3). Hence, an increasing degree of interparticle interaction yields lower ARM acquisition curves in Fig. 3. Therefore, the data in Fig. 3 indicate that the degree of magnetic interaction increased with pulse strength for all subcultures of *A. magnetotacticum*.

Studies carried out by TEM on samples from each enrichment confirmed the results shown in Fig. 3. In Fig. 4A and B, we show the morphological appearance of *A. magnetotacticum* after the 45- and 65-mT remagnetization treatments. These cells were very similar to the wild type. After 80-mT pulse remagnetization, however, we observed not only larger amounts of (coccoid) cystlike cells (15, 20) with fewer magnetosomes per cell than the vegetative cells (Fig. 4B and D) but also an increasing number of abnormal arrays of magnetosome chains (Fig. 4B through D). For better interpretation of the results presented in Fig. 3 and 4, we examined suspensions of freeze-dried whole cells on coated grids. We evaluated the average number of magnetosomes per cell, the percentage of coccoid or cystlike cells (Fig. 5), and the proportions of cells bearing normal and abnormal magnetosome chains (Fig. 6). As shown in Fig. 5, the number of magnetosomes per cell decreases slightly at a higher remagnetization pulse and the ratio of cystlike cells to normal cells increases. Whereas the total number of cells bearing magnetosomes decreases, in Fig. 6 we show that the ratio of cells bearing abnormal chains (i.e., double, crossing clumps) increases at higher remagnetization pulses. These observations are consistent with the results from the ARM studies (Fig. 3), as the increase in the frequency of abnormal magnetosome chains (Fig. 4 and 6) was accompanied by an increase in the magnetostatic interaction among the single-domain particles. We have also calculated the total cellular ferrimagnetic material content from the maximum IRM of each sample. Whereas the wild-type cells showed an iron content of 5.1% (wt/wt) in the form of magnetite, the cells exposed to higher magnetic pulses showed decreasing values from 4.8 to 2.3% for the cells treated with pulses of 55 and 80 mT, respectively. The last results are consistent with those shown in Fig. 5 and 6 as well.

DISCUSSION

The pulse remagnetization technique was used successfully for the isolation of subpopulations of *A. magnetotacticum* with higher coercivities than the wild type. As these isolated subpopulations maintained the high coercivities upon subsequent growth, it is clear that we were selecting for naturally occurring genetic variations present in the original culture from the American Type Culture Collection. Within the range of 40 to 55 mT, the remagnetization treatment does not affect the morphology of the cells, whereas higher remagnetization pulses (60 to 80 mT) induce magnetosome rearrangements and cell differentiation and increase the magnetostatic interactions. All of these effects indicate that the cellular differentiation may be triggered as a consequence of the pulse remagnetization, since the increases in magnetic interactions (Fig. 3) were correlated with the appearance of cystlike cells (Fig. 5). Culture controls for spontaneous cell differentiation were carried out (appearance of coccoid cells [20]) and showed that culture aging induced an increase in the ratio of natural cell differentiation occurrence (>1%) only after 6 to 7 weeks (9% ± 1%).

Rock magnetic theory indicates clearly that the increase in observed coercive force must be due to an increase in the volume of the individual crystals and/or an increase in the particle width-to-length ratio (6, 21). The magnetostatic force acting between two adjacent crystals, however, is proportional to the square of their magnetic moments and inversely proportional to the fourth power of their linear dimension. Hence, the effective force varies with the square of the linear dimension, and a subtle increase of particle volume, difficult to detect with TEM, could well cause the interparticle force to exceed the strength of the biological anchoring mechanisms.

We have explored this hypothesis by calculating the change of coercivity of a single-domain particle at different width/length ratios and constant volume, using the analysis of Evans and McElhinny (8) applied for a rectangular parallelepiped along the lines discussed by Butler and Banerjee

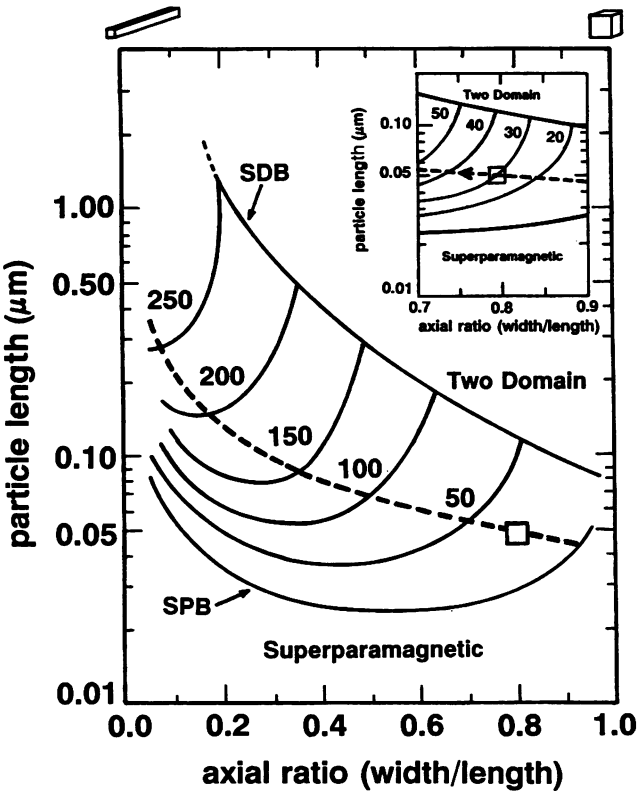

FIG. 7. Diagram of the stability of single-domain (SD) particles of magnetite. Single-domain (SDB) and superparamagnetic (SPB) stability boundaries and lengths of square cross-section parallelepipeds (in micrometers) were evaluated at various width/length ratios and coercive forces (H_b, in milliteslas) according to the analyses of Butler and Banerjee (6) and Evans and McElhinny (8). For the calculations, we assumed that the temperature was 290 K, the superparamagnetic relaxation time threshold (τ_s) was 100 s, and the spontaneous magnetization (J_s) was 480 electromagnetic units per cm^3. The SDB line defines the maximum length and width attainable by an SD particle before it changes to a two-domain particle. When SD magnetite crystals cross this boundary, the uniform magnetic spin ordering through the crystal breaks down into two or more regions (domains) with a lower net magnetostatic energy (6). The thick dashed line represents the shift of a parallelepipedlike crystal at different width/length ratios and constant volume. The average crystal volume of bacterial magnetite was assumed to be 8×10^{-14} nm^3 and is shown by the open square. The insert shows a detail of the region of the stability diagram in which the average bacterial magnetite particle is located. The arrow indicates the most probable path in the length/shape space for the SD crystal of *A. magnetotacticum* during our experiments.

(6). Figure 7 shows the location of an average fully developed single-domain crystal of bacterial magnetite (H_b = 30 mT; width/length = 0.8; length = 0.05 μm) (19). As we did not observe any significant change in size or shape of the bacterial magnetite crystal at higher coercivities, the most plausible explanation is that the crystal changed in the direction of the arrow indicated in the inset in Fig. 7. This type of displacement would render an increase in the coercivity with a minimum change in size (length) or shape (width/length), which would be difficult to detect by TEM analysis (change in length, ~5 nm; change in width/length ratio, ~0.05). This result also suggests that the major control is exerted on the volume rather than the shape. To produce the same shift in coercivity with a pure volume increase (same width/length ratio) requires a measurable increase in size which was not observed. The correlation with higher coercivities, higher magnetostatic interactions, and the appearance of abnormal magnetosome chains supports the hypothesis that intracytoplasmic structures are responsible for holding magnetosomes together.

ACKNOWLEDGMENTS

This work was supported by a grant from the Caltech Consortium in Chemistry and Chemical Engineering.

We thank M. Nesson for his helpful comments and suggestions.

REFERENCES

1. **Blakemore, R.** 1975. Magnetotactic bacteria. Science **190**:377–379.
2. **Blakemore, R. P.** 1982. Magnetotactic bacteria. Annu. Rev. Microbiol. **36**:217–238.
3. **Blakemore, R. P., R. B. Frankel, and A. J. Kalmijn.** 1980. South-seeking magnetotactic bacteria in the southern hemisphere. Nature (London) **286**:384–385.
4. **Blakemore, R. P., D. Maratea, and R. S. Wolfe.** 1979. Isolation and pure culture of a freshwater magnetic spirillum in chemically defined medium. J. Bacteriol. **140**:720–729.
5. **Blakemore, R. P., K. A. Short, D. A. Bazylinski, C. Rosenblatt, and R. B. Frankel.** 1985. Microaerobic conditions are required for magnetite formation within *Aquaspirillum magnetotacticum*. Geomicrobiol. J. **4**:53–71.
6. **Butler, R. F., and S. K. Banerjee.** 1975. Theoretical single-domain grain size range in magnetite and titanomagnetite. J. Geophys. Res. **80**:4049–4058.
7. **Cisowski, S.** 1981. Interactive vs. non-interactive single-domain behaviour in natural and synthetic samples. Phys. Earth Planet. Interiors **26**:56–62.
8. **Evans, M. E., and M. W. McElhinny.** 1969. An investigation of the origin of stable remanence in magnetite-bearing igneous rocks. J. Geomagn. Geoelectr. **21**:757–773.
9. **Fuller, M., W. S. Goree, and W. L. Goodman.** 1985. An introduction to the use of SQUIB magnetometers in biomagnetism, p. 103–151. *In* J. L. Kirschvink, D. S. Jones, and B. J. MacFadden (ed.), Magnetite biomineralization and magnetoreception in organisms. Plenum Press, New York.
10. **Gherna, R., P. Pienta, and R. Cote (ed.).** 1989. Catalogue of bacteria and bacteriophages, 17th ed., p. 18. American Type Culture Collection, Rockville, Md.
11. **Hedges, R. W.** 1985. Inheritance of magnetosome polarity in magnetotropic bacteria. J. Theor. Biol. **112**:607–608.
12. **Kalmijn, A. J., and R. P. Blakemore.** 1978. The magnetic behavior of mud bacteria, p. 355–356. *In* K. Schmidt-König and W. T. Keeton (ed.), Proceedings in life science. Animal migration, navigation and homing. Springer-Verlag KG, Berlin.
13. **Kirschvink, J. L.** 1983. Biogenic ferrimagnetism: a new biomagnetism. NATO ASI Ser. Ser. A **66**:501–531.
14. **Kirschvink, J. L.** Uniform magnetic fields and double-wrapped coil systems: improved techniques for the design of bioelectromagnetic experiments. Bioelectromagnetics, in press.
15. **Krieg, N. R.** 1976. Biology of chemoheterotrophic spirilla. Bacteriol. Rev. **40**:55–115.
16. **Lee-Whiting, G. E.** 1957. Uniform magnetic fields, p. 28. Atomic Energy of Canada, Ltd., Chalk River Project Research and Development, report CRT-673. Atomic Energy of Canada, Ltd., Chalk River, Ontario, Canada.
17. **Mann, S., R. B. Frankel, and R. Blakemore.** 1984. Structure, morphology and crystal growth of bacterial magnetite. Nature (London) **310**:405–407.
18. **Mann, S., N. H. C. Sparks, and R. P. Blakemore.** 1987. Ultrastructure and characterization of anisotropic magnetic inclusions in magnetotactic bacteria. Proc. R. Soc. Lond. B **231**:469–476.
19. **Mann, S., N. H. C. Sparks, and R. P. Blakemore.** 1987. Structure, morphology and crystal growth of anisotropic mag-

netite crystals in magnetotactic bacteria. Proc. R. Soc. Lond. B **231**:477–487.

20. **Maratea, D., and R. P. Blakemore.** 1981. *Aquaspirillum magnetotacticum* sp. nov., a magnetic spirillum. Int. J. Syst. Bacteriol. **31**:432–455.
21. **McElhinny, M. W.** 1979. Rock magnetism, p. 32–67. *In* W. B. Harland, A. H. Cook, N. F. Hughes, S. Richardson, and J. Sclater (ed.), Paleomagnetism and plate tectonics. Cambridge University Press, Cambridge.
22. **Moskowitz, B. M., R. B. Frankel, D. A. Bazylinski, and H. W. Jannasch.** 1989. A comparison of magnetite particles produced anaerobically by magnetotactic and dissimilatory iron-reducing bacteria. Geophys. Res. Lett. **16**:665–668.
23. **Moskowitz, B. M., R. B. Frankel, P. J. Flanders, R. P. Blakemore, and B. B. Schwartz.** 1988. Magnetic properties of magnetotactic bacteria. J. Magn. Magn. Mater. **73**:273–288.
24. **O'Reilly, W.** 1984. Rock and mineral magnetism. Blackie and Son Ltd., London.
25. **Petersen, N., D. G. Weiss, and H. Vali.** 1989. Magnetic bacteria in lake sediments, p. 231–241. *In* F. J. Lowes et al. (ed.), Geomagnetism and paleomagnetism. Kluwer Academic Publishers, Dordrecht, The Netherlands.
26. **Rodgers, F. G., R. P. Blakemore, N. A. Blakemore, R. B. Frankel, D. A. Bazylinski, D. Maratea, and C. Rodgers.** 1990. Intercellular structure in a many-celled magnetotactic prokaryote. Arch. Microbiol. **154**:18–22.
27. **Thompson, R., and F. Oldfield.** 1986. Environmental magnetism. Allen & Unwin Ltd., Boston.
28. **Vali, H., and J. L. Kirschvink.** 1990. Observation of magnetosome organization, surface structure, and iron biomineralization of undescribed magnetic bacteria: evolutionary speculations, p. 97–115. *In* R. B. Frankel and R. P. Blakemore (ed.), Iron biominerals. Plenum Press, New York.
29. **Wolin, E. A., M. J. Wolin, and R. S. Wolfe.** 1963. Formation of methane by bacterial extracts. J. Biol. Chem. **238**:2882–2886.